

 ${ \begin{tabular}{l} Session 4:\\ The Magellanic System: the Clouds, the Stream, and\\ the Leading Arm \end{tabular} }$ 

# Exploring the Magellanic Stellar Periphery

L. R. Cullinane<sup>1</sup>, A. D. Mackey, G. S. Da Costa<sup>2</sup>, D. Erkal<sup>3</sup> and S. E. Koposov<sup>4,5</sup>

<sup>1</sup>The William H. Miller III Department of Physics & Astronomy, Bloomberg Center for Physics and Astronomy, Johns Hopkins University, 3400 N. Charles Street, Baltimore, MD 21218 email: lcullin4@jhu.edu

 $^2{\rm Research}$ School of Astronomy and Astrophysics, Australian National University, Canberra, ACT 2611, Australia

<sup>3</sup>Department of Physics, University of Surrey, Guildford GU2 7XH, UK

<sup>4</sup>Institute for Astronomy, University of Edinburgh, Royal Observatory, Blackford Hill, Edinburgh EH9 3HJ, UK

Abstract. Recent panoramic maps of the Magellanic system have revealed a wealth of low-surface-brightness stellar substructures surrounding both the Large and Small Magellanic Clouds (LMC/SMC); clear evidence of tidal interactions between the two Clouds, as well as with the Milky Way. The Magellanic Edges Survey (MagES), a spectroscopic survey that targets red clump and red giant branch stars across the outskirts of both Clouds, aims to characterise these features and shed light on their formation. We summarise recent results from MagES, which suggest multiple previous LMC-SMC interactions are required to fully explain the observed dynamical properties of the Clouds.

Keywords. Magellanic Clouds, Local Group, Galaxies: kinematics and dynamics

## 1. Introduction

The Large and Small Magellanic Clouds (LMC/SMC) are ideally situated for detailed study of the effects of tidal interactions on galaxy evolution. The LMC is the most massive Milky Way (MW) satellite; and, despite only being on its first infall into the Milky Way's gravitational potential (Besla et al. 2007), has already significantly impacted the MW (and been affected in return). It has generated overdensities in the MW dark matter halo (e.g. Garavito-Camargo et al. 2019) and reflex motions in the MW stellar halo (e.g. Petersen and Peñarrubia 2021), and perturbed the orbits of smaller satellites and stellar streams (e.g. Erkal et al. 2019; Patel et al. 2020). In addition, dynamical models suggest the Clouds have likely repeatedly interacted with each other over several Gyr (e.g. Besla et al. 2012; Pardy et al. 2018), with signatures of these interactions long-apparent in the Clouds. The SMC is particularly disturbed, with an asymmetric, irregular morphology; line-of-sight (LOS) depths up to 30 kpc (e.g. Hatzidimitriou and Hawkins 1989; Nidever et al. 2013); and kinematic evidence for tidal expansion (De Leo et al. 2020; Zivick et al. 2021). While more ordered than the SMC, the LMC also displays substantial disturbances, including multiple warps (Olsen and Salvk 2002; Choi et al. 2018), and a tilted, off-centre stellar bar (van der Marel and Cioni 2001).

Recently, deep photometric studies of the Magellanic periphery (e.g. Mackey et al. 2016, 2018; Pieres et al. 2017), in combination with multidimensional phase-space information from Gaia (e.g. Belokurov and Erkal 2019; Gaia Collaboration et al. 2021b),

<sup>&</sup>lt;sup>5</sup>Institute of Astronomy, University of Cambridge, Madingley Road, Cambridge CB3 0HA, UK

<sup>©</sup> The Author(s), 2025. Published by Cambridge University Press on behalf of International Astronomical Union. This is an Open Access article, distributed under the terms of the Creative Commons Attribution licence (https://creativecommons.org/licenses/by/4.0/), which permits unrestricted re-use, distribution and reproduction, provided the original article is properly cited.

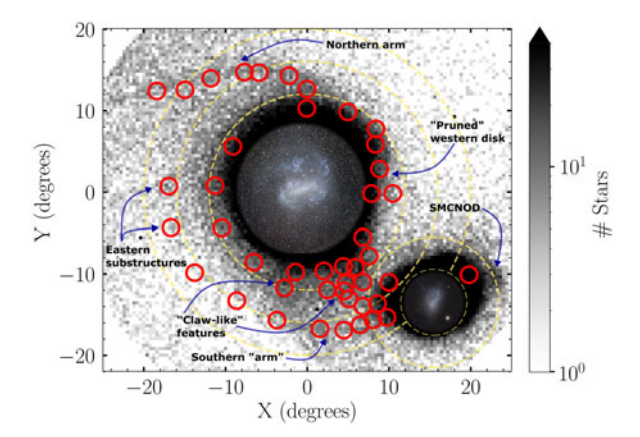


Figure 1. Density map of Magellanic red clump/RGB stars selected from Gaia EDR3, using the criteria of (Cullinane et al. 2022), with major features labelled. Red circles indicate the position of MagES 2-degree diameter fields. Dashed yellow circles indicate distances of  $12^{\circ}/16^{\circ}/20^{\circ}$  from the LMC and  $4^{\circ}/8^{\circ}$  from the SMC centres respectively.

have also revealed a wealth of low-density stellar substructure surrounding both Clouds (Fig. 1). This includes a  $\sim 23^\circ$  long arm-like feature north of the LMC (Mackey et al. 2016; Belokurov and Erkal 2019) and diffuse structures to the east of the LMC (El Youssoufi et al. 2021), claw-like structures in the southern LMC outskirts and an apparent truncation in the western edge of the LMC disk (Mackey et al. 2018), diffuse overdensities north of the SMC (Pieres et al. 2017; El Youssoufi et al. 2021), and a long thin feature which appears to wrap around the southern LMC, stretching between the eastern outskirts of the SMC and the eastern LMC disk (Belokurov and Erkal 2019). These extended features are of particular interest in constraining the interaction history of the Clouds: stars at large radii are more weakly gravitationally bound, and thus relatively easily perturbed by interactions compared to stars in the central regions of the galaxies; and, because dynamical timescales in the outskirts are long, the resulting structural and kinematic signatures are more persistent compared to the central regions, potentially remaining for several Gyr.

However, in order to place precise constraints on the complex interactions which produce these features, full three-dimensional (3D) kinematic data are critical. With the advent of the Gaia satellite, providing proper motions for stars  $G\lesssim 21$  mag across the entire Magellanic system (Gaia Collaboration et al. 2018), the limiting factor are now line-of-sight (LOS) velocities. Existing spectroscopic surveys of the Clouds have predominantly targeted stars in their interior; and the vast majority of stars in the low-density outskirts are too faint for Gaia to provide LOS velocities (available only for  $G\lesssim 14$  mag: Gaia Collaboration et al. 2022). The Magellanic Edges Survey (MagES), a spectroscopic survey which specifically targets the low-density periphery of the Clouds, is designed to fill this gap. Here, we summarize recent results from MagES, and how those inform our understanding of the masses, orbits, and interaction history of the Clouds.

## 2. The Magellanic Edges Survey

MagES utilizes the 2dF multi-object fibre positioner (Lewis et al. 2002), and the dual-beam AAOmega spectrograph (Sharp and Birchall 2010) on the 3.9 m Anglo-Australian Telescope (AAT). The 2dF positioner allows for the observation of  $\sim 350$  science targets per 2-degree-diameter field. We configure the blue arm on AAOmega with the 1500 V grating (wavelength coverage  $\sim 4910-5615$  Å and resolution R $\sim 3700$ ), designed to provide

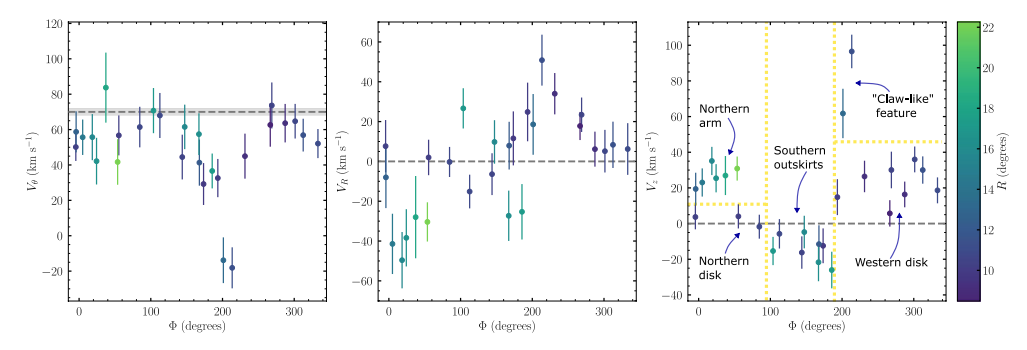


Figure 2. Aggregate kinematics relative to the plane of the LMC disk for MagES fields analysed to date (compiled from Cullinane et al. 2021, 2022), calculated assuming a disk inclination of  $i=36.5^{\circ}$  and line-of-nodes position angle  $\Omega=145^{\circ}$  (Cullinane et al. 2022). Fields associated with distinct regions are labelled as in Fig. 1 and separated by dashed yellow lines in the right panel. From left to right, the azimuthal velocity  $V_{\theta}$ , the in-plane radial velocity  $V_R$ , and the out-of-plane (vertical) velocity perpendicular to the disk plane  $V_z$  are shown, each plotted as a function of position angle east of north. Points are coloured by LMC on-sky galactocentric radius. Grey dashed lines indicate predicted kinematics for an equilibrium disk.

precise LOS velocity estimates using the MgIb triplet. The red arm is configured with the 1700D grating (wavelength coverage  $\sim\!8370\!-\!8790$  Å and resolution of R $\sim\!10000$ ), designed to provide sufficiently high-resolution coverage of the CaII triplet to allow for an estimation of metallicity (as in e.g. Da Costa 2016) and a complementary LOS velocity estimate.

Fourty-four MagES fields have been observed to date; their locations are indicated in Fig. 1. Within each field, MagES targets red clump and red-giant branch (RGB) stars selected from a combination of Dark Energy Camera (DECam) photometry (Koposov et al. 2015; Mackey et al. 2018) if observed prior to the release of Gaia DR2, and Gaia DR2/EDR3 photometry (Gaia Collaboration et al. 2018, 2021a) for fields observed subsequent to these data releases. In total, LOS velocities have been obtained for > 12000 such stars, with metallicity estimates for > 500 RGB stars with G < 18 mag. For the more numerous and fainter red clump stars within each field, we stack spectra for likely ( $P \ge 50\%$ ) Magellanic stars to create a single "representative" spectrum used for these measurements; the resulting [Fe/H] estimates tend towards the mean field metallicity. In addition, as the red clump is a standardizable candle, we utilize this to obtain relative mean distance estimates for fields which contain similar stellar populations, as indicated by having consistent mean metallicities and  $G_{BP} - G_{RP}$  colours.

As it is generally informative to consider the kinematics and distances of MagES fields relative to the frame of the LMC disk, we utilize the framework presented in van der Marel et al. (2002) to transform the observed kinematics of each field into a cylindrical coordinate system aligned with the LMC disk, with its origin at the LMC centre of mass (COM). We subsequently obtain  $V_{\theta}$ , the azimuthal rotation velocity (positive values indicate motion in the same direction as the LMC's clockwise on-sky rotation);  $V_R$ , the in-plane radial velocity (positive values indicate motion radially outward from the COM in the plane of the disk);  $V_z$ , the vertical velocity perpendicular to the disk plane (positive values indicate motion in a direction predominantly towards the viewer: i.e. "in front of" the disk plane); as well as dispersions  $(\sigma_{\theta}, \sigma_R, \sigma_z)$  in each of these components. We additionally obtain the out-of-plane distance z, describing how far "in front of" or "behind" the expected disk plane stars in each field are located. Fig. 2 presents these measurements for MagES fields analysed to date (i.e. observed prior to 2022) which are associated with the LMC.

## 2.1. Magellanic Models

In order to assist in our interpretation of the disturbed kinematics in the Magellanic outskirts, we compare our observations to a suite of simple dynamical models of the LMC+SMC+MW system. These models are only a first exploration of the large and complex parameter space that describes the allowable orbits of the Clouds, and there are consequently associated limitations: most significantly a lack of self-gravity. This can affect both the orbits of the Clouds, and the response of stars within them to close interactions; accordingly, we only perform qualitative comparisons to our observations.

The LMC is modelled as a collection of test particles within a two-component potential: an exponential disk with mass  $2\times 10^9~\rm M_{\odot}$ , scale radius 1.5 kpc, and scale height 0.4 kpc; and a Hernquist dark matter halo (Hernquist 1990) of mass  $1.5\times 10^{11}~\rm M_{\odot}$  (Erkal et al. 2019) and scale radius 20 kpc, such that the circular velocity is  $\sim 90~\rm km~s^{-1}$  at 10 kpc. The SMC is modelled as a Hernquist profile with mass  $2.5\times 10^9~\rm M_{\odot}$  and scale radius 0.043 kpc, such that it has a circular velocity of 60 km s<sup>-1</sup> at 2.9 kpc (Stanimirović et al. 2004). The Milky Way is modelled as a three-component system with a bulge, disk, and dark matter halo similar to Bovy (2015). We treat each of these three galaxies as a particle sourcing a potential, allowing us to account for the motion of the Milky Way in response to the LMC (Gómez et al. 2015) and the dynamical friction of the Milky Way on the LMC (Jethwa et al. 2016). The LMC and SMC are initialized at their present day locations, then rewound for one Gyr in the presence of each other and the Milky Way. The LMC disk is then initialized with  $\sim 2.5\times 10^6$  tracer particles† using AGAMA (Vasiliev 2019) to account for the LMC's velocity dispersion, with a geometry matching that from Cullinane et al. (2022). The system is then evolved to the present.

We run multiple model realizations, sampling from literature uncertainties on the current-day systemic properties of both the LMC and SMC, to explore the allowable parameter space, and hence differing orbits (and interaction histories) for the Clouds. In all model realizations, the SMC has had a recent close pericentric passage around the  $LMC \sim 150 \text{ Myr}$  ago (consistent with Zivick et al. 2018), with a total pericentric distance  $r_{\rm peri} \sim 8.0 \ {\rm kpc}$  (consistent with Choi et al. 2022). The projected galactocentric radius of the pericentric passage is  $\sim 4$  kpc, in a direction toward the south-west of the LMC. At earlier times, the orbit of the SMC varies significantly depending on how the systemic motions of both Clouds are sampled. Approximately half our realizations have a second SMC crossing of the LMC disk  $\sim 400$  Myr ago, which can occur across a broad range  $(\sim 29 \pm 10 \text{ kpc})$  of in-plane radial distances. A handful of model realizations  $(\sim 4\%)$  also have a roughly simultaneous third disk crossing and SMC pericentric passage  $\sim 1$  Gyr ago, though a significantly larger fraction would experience one or both of the disk crossing and pericentric passage if our models were rewound for a greater length of time than precisely one Gyr. The particulars of this interaction are much less robustly constrained than more recent interactions, with pericentric distances  $r_{\rm peri} \sim 6 \pm 3$  and crossing distances of  $\sim 54^{+13}_{-46}$  kpc permitted due to the increasing uncertainty in the SMC's orbit at earlier times. Fig. 3 shows the current particle distribution for a single model realisation which has experienced each of these interactions, coloured by the particle distance from the SMC at the time of each SMC crossing of the LMC disk plane, indicating which regions of the LMC are most strongly affected by each interaction.

## 3. Properties of the Magellanic outskirts

Below, we summarize recent results from MagES, as published in Cullinane et al. (2020, 2021, 2022, 2023), and their implications for the interaction history of the Clouds.

† We do not initialize the SMC potential with tracer particles.

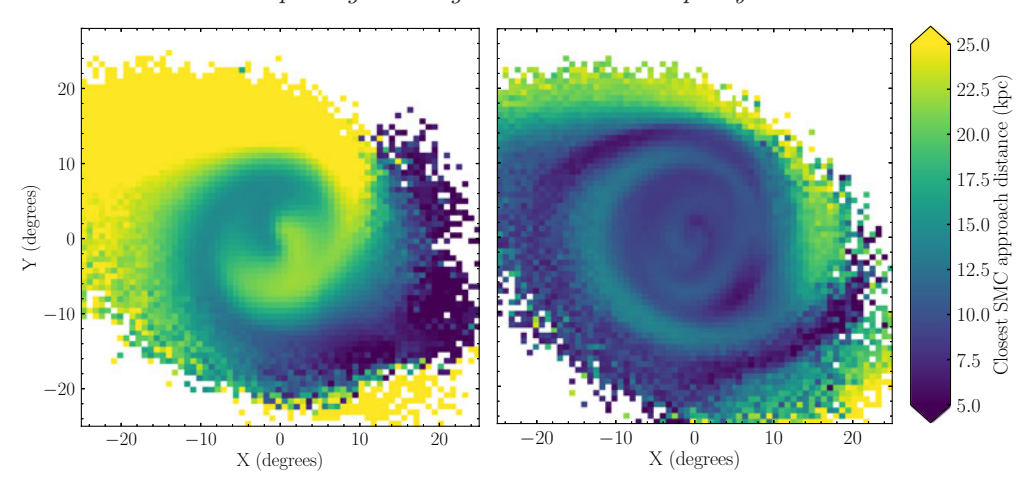


Figure 3. Current particle distribution for a single Magellanic model realisation, colour coded by the particle distance from the SMC at the time of the SMC disk crossings  $\sim 400$  Myr ago (left) and  $\sim 980$  Myr ago (right). Adapted from Cullinane et al. (2022).

## 3.1. The northern LMC and its tidal arm

MagES fields across the northeastern disk of the LMC display very ordered kinematics, with aggregate out-of-plane distances, vertical and radial velocities consistent with zero, and azimuthal velocities of  $\sim 70$  km s<sup>-1</sup>. This is consistent with previous measurements of the LMC's rotation derived from data at smaller radii (e.g. van der Marel and Kallivayalil 2014). Under the assumption that this indicates equilibrium kinematics within these fields, we thus utilize the derived circular velocity to calculate the enclosed mass of the LMC within 10.5 kpc as  $M_{\rm enc} = (1.8 \pm 0.3) \times 10^{10} \ {\rm M}_{\odot}$ . This is consistent with enclosed mass measurements derived using similar techniques at smaller radii when projected to the same distance, but low compared to mass measurements derived using more indirect methods ( $\sim 1.5 - 3 \times 10^{11} \ \mathrm{M}_{\odot}$ ), such as perturbations to stellar streams (e.g. Erkal et al. 2019), the timing argument (Peñarrubia et al. 2016), or cosmological simulations of similar systems (e.g. Shao et al. 2018). This difference is to be expected, as each of the above methods provides the total infall mass of the LMC, including its dark halo; in contrast, the MagES fields here are still well within the LMC's dark halo. If, however, the assumption is made that the LMC rotation curve remains flat out to  $\sim 30$  kpc (where LMC-associated stars have been found: Navarrete et al. 2019), and that the LMC is embedded in a typical dark matter halo, the inferred enclosed mass is  $\sim 1.1 \times 10^{11} \text{ M}_{\odot}$ : more in line with total infall mass estimates.

Fields along the LMC's northern tidal arm have similar metallicities to those of the northern LMC disk, with a mean overall metallicity of  $[Fe/H] \sim -1$ , and only weak  $(<2\sigma)$  evidence for a negative metallicity gradient along the feature. The azimuthal velocity along the arm is broadly consistent with the LMC's rotation, and distance estimates also suggest the arm largely follows the inclined LMC disk plane. In combination, this suggests the arm is comprised of LMC disk material. There are, however, strong non-equilibrium motions in the radial and vertical velocity components: the radial velocity is consistently strongly negative, moving at  $\geq 30$  km s<sup>-1</sup> inward along the arm, and the vertical velocity gradually increases along the feature from near zero to a maximum of nearly 30 km s<sup>-1</sup> in the most distant field. The increasing vertical velocity is a result of the LMC's infall to the MW potential: the orbit and inclination of the LMC relative to the Milky Way is such that the MW's gravitational force acts in a direction predominantly aligned with the positive z direction, and models including only the LMC+MW are able to replicate

the observed trend. However, the strongly negative radial velocity cannot be replicated in our LMC+MW models, and likely requires perturbation from the SMC.

Of the several LMC-SMC interactions which our models indicate could potentially impact the LMC and hence contribute to the formation of the northern arm, only the SMC disk crossing and pericentric passage  $\sim 1$  Gyr ago closely affects stars which are today in the vicinity of the northern arm, as seen in Fig. 3. The most recent pericentric passage, although a close interaction, occurs effectively diametrically opposite to the northern arm, and – as dynamical timescales at the large radius of the northern arm are  $\gtrsim 1$  Gyr – insufficient time has passed for debris disturbed by this interaction to reach the position of the northern arm. The  $\sim 400$  Myr disk crossing most closely affects stars in the western outskirts of the LMC. We therefore suggest the interaction  $\sim 1$  Gyr ago (or potentially older interactions not captured in our current models) have likely contributed to the formation of the northern arm.

#### 3.2. The disturbed southern LMC

MagES fields throughout the southern outskirts of the LMC have metallicities consistent with the northern LMC disk, indicating these are also dominated by LMC material. However, unlike the ordered kinematics of the northeastern disk, the kinematics in this region are quite disturbed, with all fields displaying clear kinematic trends as a function of position angle. Moving toward the southwest, the azimuthal velocity substantially decreases, to  $\sim 30 \text{ km s}^{-1}$ , and the out-of-plane distance increases significantly, with the outermost fields located up  $\sim 12 \text{ kpc}$  closer to us than the nominal disk plane. However, the vertical velocity in these fields is generally mildly negative ( $|V_z| \lesssim 20 \text{ km s}^{-1}$ ), indicating material in these fields is currently slowly moving back towards the disk plane.

Fields at smaller LMC galactocentric radii  $(R \sim 10^{\circ})$  show a trend of increasing inplane radial velocity as a function of increasing position angle, indicating an increasingly strong radially outward motion as one approaches the present position of the SMC. Our models suggest any of the potential LMC-SMC interactions in the past Gyr can produce this trend. In contrast, fields at larger LMC galactocentric radii  $(R \sim 16^{\circ})$ , including fields nominally along the "southern arm") have increasingly negative in-plane radial velocities as a function of position angle. This is most closely replicated by models which have experienced multiple LMC-SMC interactions in the past Gyr, including disk crossings both  $\sim 1$  Gyr and  $\sim 400$  Myr ago.

Unlike the relatively well-defined kinematic trends observed in the southern outskirts, fields located in the western "claw-like" feature are highly disturbed. With a negative  $V_{\theta}$  observed, this structure appears to be counter-rotating relative to the LMC disk; and it posses enormous out-of-plane velocities ( $V_z > 60 \text{ km s}^{-1}$ ), indicating it is rapidly moving towards us and further away from the LMC disk plane. Our current Magellanic models cannot replicate these distinctive kinematics, requiring further investigation into the origin of this feature.

## 3.3. The pruned western LMC disk

Fields along the western outskirts of the LMC also display largely consistent kinematic trends. Fields in the southwest, nearest the present-day position of the SMC, have comparable in-plane radial velocities to the nearby southern disk fields at similar radii, suggesting these fields may be similarly perturbed by LMC-SMC interactions in the past Gyr. More northern fields have in-plane radial velocities consistent with zero. Fields throughout the western outskirts are located on average  $\sim 4~\rm kpc$  in front of the LMC disk plane, and have moderately positive vertical velocities ( $V_z \sim 15-35~\rm km~s^{-1}$ ) indicating this region of the disk continues to move towards us and away from the LMC disk plane

(though significantly more slowly than the claw-like features). While our models suggest stars in the western LMC outskirts may be closely affected by a SMC disk crossing  $\sim 400$  Myr ago, with resulting in-plane radial velocities similar to those observed, our models also predict kinematic trends in the vertical direction which are opposite to those that we observe: i.e. increasingly negative out-of-plane distances and vertical velocities in the northwestern LMC. More detailed modelling of this disk crossing is required in order to determine if there are associated parameters which can reproduce our observed kinematic trends, or if earlier interactions with the SMC are responsible for the largely positive vertical perturbations we observe.

## 3.4. The extreme eastern SMC

MagES fields in the outskirts of the SMC  $(R_{\rm SMC} \sim 6^{\circ})$  have distinctly lower metallicities ( $[Fe/H]\sim -1.6$ ) than fields in the greater LMC outskirts, suggesting they are indeed dominated by perturbed SMC material, and have kinematics reflective of the SMC's tidal expansion observed at smaller radii (e.g. De Leo et al. 2020). However, at greater distances, the situation is more complex. In MagES field 3, located  $\sim 9^{\circ}$  east of the SMC along the "southern arm" feature, two chemodynamically distinct populations are observed. Approximately two-thirds of the stars in this field have kinematics and metallicities consistent with those expected for extended SMC debris. In contrast, the remaining ~one-third of the material in this field is substantially more metal-rich ( $[Fe/H] \sim -1.2$ ), located  $\gtrsim 7$  kpc closer to us than the bulk population, and is moving away from the SMC significantly more rapidly ( $V_{\rm rel} \sim 230 \; {\rm km \; s^{-1}}$ , compared to  $\sim 70 \; {\rm km \; s^{-1}}$  for the bulk population) in a direction largely toward the LMC. While an association with the LMC cannot be ruled out given the higher metallicity of this population, this population does have substantially different kinematics from nearby MagES fields dominated by LMC debris. This material may instead by debris from the inner (i.e. more metal-rich) SMC, which has been recently perturbed by, e.g., the SMC's close pericentric passage around the LMC  $\sim 150$  Myr ago.

## 4. Summary

The Magellanic Clouds are ideal testbeds in which to study the effects of interactions on galaxy structure, kinematics, and star formation. Each distinct feature in the wealth of substructure spanning the outskirts of the Clouds encodes unique constraints on their past interactions, with multidimensional phase-space information required in order to unravel these complex and often overlapping signatures. MagES has already made great strides in characterising the properties of multiple Magellanic substructures, and has demonstrated the efficacy of such data as a benchmark for assessing dynamical models to disentangle their origins, finding multiple LMC-SMC interactions are likely required to produce the disturbed features observed. Additional observations from MagES and forthcoming surveys – such as the 4-metre Multi-Object Spectroscopic Telescope (4MOST) consortium survey 1001 Magellanic Fields (1001MC: Cioni et al. 2019) – in conjunction with more detailed dynamical modelling, will allow for the interaction history of the Clouds to be precisely constrained, and provide new understanding on how these processes have shaped their evolution.

#### References

Belokurov, V. & Erkal, D. 2019, MNRAS, 482(1), L9–L13.
Besla, G., Kallivayalil, N., Hernquist, L., et al. 2007, ApJ, 668(2), 949–967.
Besla, G., Kallivayalil, N., Hernquist, L., et al. 2012, MNRAS, 421(3), 2109–2138.
Bovy, J. 2015, ApJS, 216(2), 29.

Choi, Y., Nidever, D. L., Olsen, K., et al. 2018, ApJ, 866(2), 90.

Choi, Y., Olsen, K. A. G., Besla, G., et al. 2022, ApJ, 927(2), 153.

Cioni, M.-R., Storm, J., Bell, C. P. M., et al. 2019, The Messenger, 175, 54-57.

Cullinane, L. R., Mackey, A. D., Da Costa, G. S., et al. 2021, MNRAS, 510(1), 445-468.

Cullinane, L. R., Mackey, A. D., Da Costa, G. S., et al. 2022, MNRAS, 512(4), 4798-4818.

Cullinane, L. R., Mackey, A. D., Da Costa, G. S., et al. 2020, MNRAS, 497(3), 3055–3075.

Cullinane, L. R., Mackey, A. D., Da Costa, G. S., et al. 2023, MNRAS, 518, L25-L30.

Da Costa, G. S. 2016, MNRAS, 455(1), 199–206.

De Leo, M., Carrera, R., Noël, N. E. D., et al. 2020, MNRAS, 495(1), 98–113.

El Youssoufi, D., Cioni, M.-R. L., Bell, C. P. M., et al. 2021, MNRAS, 505(2), 2020–2038.

Erkal, D., Belokurov, V., Laporte, C. F. P., et al. 2019, MNRAS, 487(2), 2685–2700.

Gaia Collaboration, Brown, A. G. A., Vallenari, A., et al. 2018, A&A, 616, A1.

Gaia Collaboration, Brown, A. G. A., Vallenari, A., et al. 2021, a A&A, 649a, A1.

Gaia Collaboration, Luri, X., Chemin, L., et al. 2021,b A&A, 649b, A7.

Gaia Collaboration, Vallenari, A., Brown, A., et al. 2022, A&A,.

Garavito-Camargo, N., Besla, G., Laporte, C. F. P., et al. 2019, ApJ, 884(1), 51.

Gómez, F. A., Besla, G., Carpintero, D. D., et al. 2015, ApJ, 802(2), 128.

Hatzidimitriou, D. & Hawkins, M. R. S. 1989, MNRAS, 241(4), 667–690.

Helmi, A., Irwin, M., Deason, A., et al. 2019, The Messenger, 175, pp. 23-25.

Hernquist, L. 1990, ApJ, 356(2), 359.

Jethwa, P., Erkal, D., & Belokurov, V. 2016, MNRAS, 461(2), 2212–2233.

Koposov, S. E., Belokurov, V., Torrealba, G., & Evans, N. W. 2015, ApJ, 805(2), 130.

Lewis, I. J., Cannon, R. D., Taylor, K., et al. 2002, MNRAS, 333(2), 279-298.

Mackey, A. D., Koposov, S. E., Erkal, D., et al. 2016, MNRAS, 459(1), 239-255.

Mackey, D., Koposov, S. E., Da Costa, G., et al. 2018, ApJ, 858(2), L21.

Navarrete, C., Belokurov, V., Catelan, M., et al. 2019, MNRAS, 483(3), 4160-4174.

Nidever, D. L., Monachesi, A., Bell, E. F., et al. 2013, ApJ, 779(2), 145.

Olsen, K. A. G. & Salyk, C. 2002, AJ, 124(4), 2045–2053.

Pardy, S. A., D'Onghia, E., & Fox, A. J. 2018, ApJ, 857(2), 101.

Patel, E., Kallivayalil, N., Garavito-Camargo, N., et al. 2020, ApJ, 893(2), 121.

Peñarrubia, J., Gómez, F. A., Besla, G., et al. 2016, MNRAS, 456(1), L54-L58.

Petersen, M. S. & Peñarrubia, J. 2021, Nature Astronomy, 5(3), 251–255.

Pieres, A., Santiago, B. X., Drlica-Wagner, A., et al. 2017, MNRAS, 468(2), 1349–1360.

Shao, S., Cautun, M., Deason, A. J., et al. 2018, MNRAS, 479(1), 284–296.

Sharp, R. & Birchall, M. N. 2010, PASA, 27(1), 91–103.

Stanimirović, S., Staveley-Smith, L., & Jones, P. A. 2004, ApJ, 604(1), 176–186.

van der Marel, R. P., Alves, D. R., Hardy, E., & Suntzeff, N. B. 2002, AJ, 124(5), 2639–2663.

van der Marel, R. P. & Cioni, M.-R. L. 2001, AJ, 122(4), 1807–1826.

van der Marel, R. P. & Kallivayalil, N. 2014, ApJ, 781(2), 121.

Vasiliev, E. 2019, MNRAS, 482(2), 1525-1544.

Zivick, P., Kallivayalil, N., & van der Marel, R. P. 2021, ApJ, 910(1), 36.

Zivick, P., Kallivayalil, N., van der Marel, R. P., et al. 2018, ApJ, 864(1), 55.

## Discussion

SIMON ROZIER: Do you account for the reflex motion of the LMC to the SMC in your simulations?

LARA CULLINANE: Yes, though we do not account for dynamical friction between the Clouds.

JOANNA SAKOWSKA: Can you tell me more about how you classified the chemodynamically distinct stars near the SMC to have come from the inner SMC? Have you done any age dating?

LARA CULLINANE: We found these stars were more noticably more metal-rich, with a mean [Fe/H] of  $\sim -1.2$ , than the bulk population in this field. Comparing that to the SMC's current metallicity gradient suggests these stars could have originated in the inner SMC and very recently been pushed outwards. The relatively high velocity of this population suggests that scenario is not implausible, but more detailed models are needed to confirm this. We have not yet done any age-dating for this population, but this is something we are interested in pursuing.

JIANLING WANG: The Northern tidal arm is so thin from your results. It looks like it is crossing the Galactic disk, do you have any plan to identify and make spectral observations of these stars above the Galactic disk? These stars will be important for constraining the modelling.

LARA CULLINANE: We did previously plan to follow up those stars, but were unfortunately weathered out during the observing run; we may revisit this in the future. Stars along the northern arm will also be followed up in the 4MOST consortium surveys 1001MC (Cioni et al. 2019) and the Milky Way Halo Low-Resolution Survey (Helmi et al. 2019).

YANBIN YANG: I am very interested in the thin tail north of the LMC. Do you have any information like stellar ages or metallicities for it?

LARA CULLINANE: We do not have ages for these stars, but we are interested in measuring these in the future. We do, however, have metallicities derived from the equivalent width of the Calcium triplet, and find mean [Fe/H] values of  $\sim -1$  along the entire arm.